Arch Bridges
ARCH´04
P. Roca and E. Oñate (Eds)

NONLINEAR SEISMIC ANALYSIS OF THE SECOND SAIKAI BRIDGE -CONCRETE FILLED TUBULAR (CFT) ARCH BRIDGE-

H. Fujita[*], Q. Wu[*], M. Yoshimura[†], K. Takahashi[*], S. Nakamura[*] and K. Furukawa[††]

[*] Department of Civil Engineering, Faculty of Engineering
Nagasaki University
1-14, Bunkyo-machi, Nagasaki, Japan
e-mail: takahasi@civil.nagasaki-u.ac.jp

[†]Nagasaki Shipyard & Machinery Works
Mitsubishi Heavy Industries, LTD.,
1-1, Akunoura-cho, Nagasaki, Japan
Email: mitsuhiro_yoshimura@mhi.co.jp

[††]Civil Engineering Information Office, Public Works Department
Nagasaki Prefectural Government
2-13 Edo-machi, Nagasaki, Japan

Key words: Concrete filled steel tube, arch bridge, nonlinear seismic response, Second Saikai Bridge

Abstract. *The technology of concrete filled steel tubes (CFT) arch bridges has developed rapidly in China since 1990. More than one hundred CFT arch bridges have been built or are now under construction. However, since the weight of a CFT arch rib is greater than that of a steel rib and the arch action is not effective in the out-of-plane direction, the seismic safety of CFT bridges should be evaluated. This paper examines the free vibrations and nonlinear seismic responses of the Second Saikai Bridge. The first CFT arch bridge to be built in Japan, this bridge has a main span length of 240m. The natural vibration characteristics of this bridge are discussed using a three-dimensional FE model. A nonlinear seismic analysis is performed using the strong ground motions observed in the Hyogo-ken Nanbu Earthquake of Japan. The nonlinear seismic characteristics and seismic safety of this bridge are examined in detail by subjected the bridge to earthquakes in the out-of-plane direction. Seismic safety can be confirmed because the strains in the infilled concrete of the arch rib do not reach to the yield strains and the curvatures of the piers are within the permitted curvatures.*

1 INTRODUCTION

Concrete filled steel tubes (CFT) constructions have advantages over either whole steel tube members or reinforced concrete members. The infilled concrete delays local buckling of the steel tube, and the steel tube reinforces the concrete to resist tension, bending moment, and shear force. The tube also acts as a formwork for the concrete during construction of the bridge, thus saving a major construction cost[i,ii], and the composite structural action between the infilled concrete and the steel tube improves the member's load-carrying capacity. As a result of these advantages, CFT construction for bridges has become widespread in recent decades[iii,iv].

In arch bridges, it may be practical to use concrete filled steel tubes for arch ribs in which the compression axial force is predominant. The technology of CFT arch bridges has developed rapidly in China since 1990, and more than one hundred CFT arch bridges have been built or are now under construction[v,vi,vii,viii]. The Second Saikai Bridge, the first CFT arch bridge in Japan, is under construction in Nagasaki Prefecture.

The CFT arch bridge is a rational choice in China, where there is only a slight possibility of strong earthquakes occurring. In Japan, the seismic safety of CFT arch bridges must be examined, since the Hyogo-ken Nanbu Earthquake, the ductility of bridges has severely been required[ix,x]. In the Design Specification for Highway Bridges 1996[ix], the safety of bridges with complex dynamic responses must be checked using two types of ground motions. The first is the plate-boundary-type earthquakes (Type I) having a magnitude of about 8, and the second is the Inland-type earthquakes (Type II) having a magnitude of about 7-7.2 at very short distance. Since the weight of a CFT arch rib is greater than that of a steel rib and the arch action is not effective in the out-of-plane direction, the effect of a large earthquake force in the out-of-plane direction on CFT arch bridges is a cause of concern.

The seismic properties for CFT arch bridges have been the subjects of recent research. Liu et al.[xi,xii,xiii] analyzed the seismic response characteristics of two CFT arch bridges in China and clarified the nonlinear seismic performance of the tentatively designed CFT arch bridges. Wu et al.[xiv] examined the effect of the filled concrete length on the nonlinear seismic response of arch bridge (Sanqian Bridge in China) in which the tubes are only partially filled with concrete. Until now, however, the nonlinear seismic response of an actual CFT arch bridge in Japan has seldom been examined. Especially, the seismic safety of a CFT arch bridge may be examined under strong ground motions.

This paper focuses on the free vibrations and nonlinear seismic responses of the Second Saikai Bridge, which is the first CFT arch bridge in Japan. This bridge has a main span length of 240m. A three-dimensional FE model is used in the analysis. The natural vibration characteristics of this bridge are first discussed, then, a nonlinear seismic analysis is performed using the strong ground motions recommended in the Design Specification for Highway Bridges 1996[ix]. The bridge is subjected to these earthquakes in the out-of-plane direction and the longitudinal direction. The axial force fluctuation and the non-linearity of the biaxial bending moments of the CFT arch rib are taken into account by using fiber model. The nonlinear seismic characteristics and seismic safety of this bridge are examined by directly integrating the nonlinear differential equations of motion.

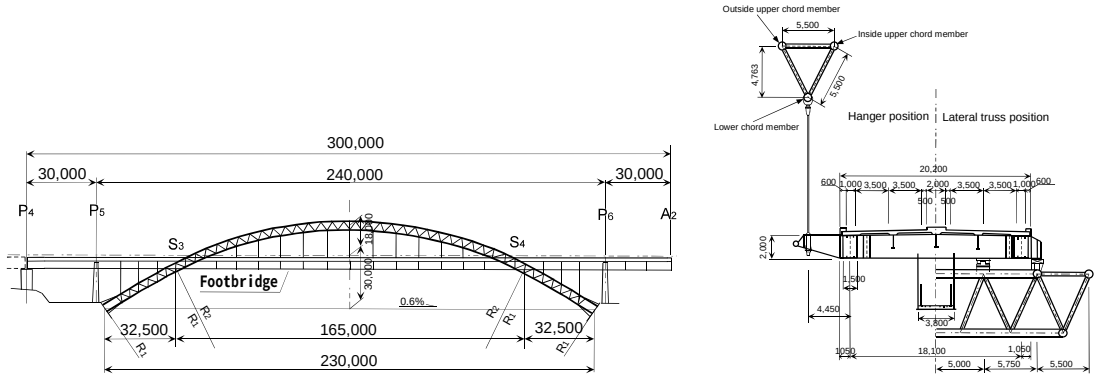

Figure 1: General view of the Second Saikai Bridge (unit: mm)

2 A BRIEF DESCRIPTION OF THE SECOND SAIKAI BRIDGE

The Second Saikai Bridge (tentative name) is a highway bridge on the Nishisonogi Region Expressway. The bridge crosses the Harioseto channel, connecting the Sasebo urban area and the Nagasaki urban area. The bridge is scheduled to be completed in 2005.

As shown in Figure 1, the main span is 240m in length and the side spans are 30m in length. The bridge is 20.2m in width. The landscape of the site, the need to harmonize the design with that of the present Saikai Bridge (a deck type steel arch bridge with a span of 216m, completed in 1955) and the need to reduce the bridge's construction costs together lead the selection of the half-though braced-rib CFT arch bridge design for the main span. The bridge has two parallel arch ribs, each of which has a triangular cross-section consisting of three steel tubes (outside upper chord member, inside upper chord member and lower chord member). High fluidity concrete fills the three steel tubes. The three steel tubes have an 812.8mm outer diameter and a thickness that differs depending upon the position of the arch rib. The deck system consists of I-beams arranged longitudinally, upon which a concrete slab is placed.

A footbridge is suspended by strand ropes and steel tubes under the bridge. The footbridge allows pedestrians to cross the Second Saikai Bridge and visit the public park. The footbridge is 293.225m long and 3m wide. The footbridge itself is an H-beam steel girder.

3 ANALYTICAL MODEL

The three-dimensional FE model that is used in this study. The arch rib, stiffening girder, lateral bracing, and pier are all modeled using three-dimensional beam elements based on actual cross-sectional properties. The column and hanger are modeled using three-dimensional truss elements. The lump mass matrix is adopted for this analysis. The cross beam and lateral beam take into account the stiffness of the floor system, and the stiffening girder takes into account the weights of floor system and footbridge.

Regarding boundary conditions, the springing position of the arch rib and the pier bases are fixed in all degrees of freedom. The earthquake shear force distribution rubber bearings are installed in the joints between the stiffening girder and the piers (P4, P5 and P6), in the joints between the stiffening girder and the abutment A2, and in the joints between the stiffening

Table 1: Natural Frequencies, effective masses and modal shapes

No.	Natural Freq. (Hz)	Effective masses			Modal shape
		x direction	y direction	z direction	
1	0.365	0.0000	0.0000	81.9841	
2	0.470	-95.3952	0.0379	0.0000	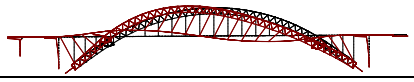
3	0.473	-5.8094	-1.1373	0.0000	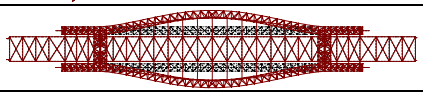
4	0.574	0.0000	0.0000	-36.0222	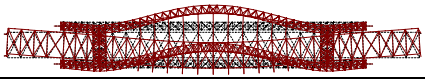
5	0.640	-14.0905	0.3460	0.0000	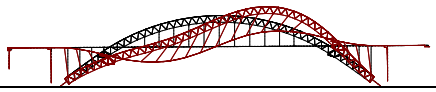
6	0.683	0.0000	0.0000	-0.9349	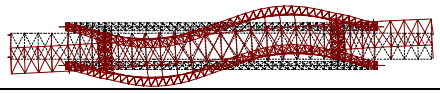
7	0.833	0.0000	0.0000	-0.6934	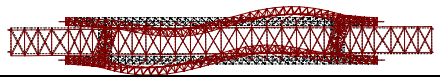
8	0.850	0.0000	0.0000	57.2035	
9	0.927	0.0460	23.4554	0.0000	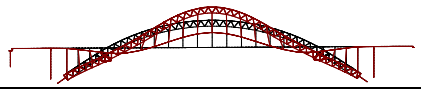

girder and the lateral beams (S3 and S4). Linear springs are used to simulate them.

4 NATURAL VIBRATION CHARACTERISTICS

The natural frequencies, effective masses and modal shapes of the Second Saikai Bridge are summarized in Table 1.

Regarding in-plane natural vibrations, the first natural vibration, which has a frequency of 0.470Hz, corresponds to the floating mode, like that of cable-stayed bridges. This is due to the installation of the earthquake shear force distribution rubber bearings in the longitudinal direction of the bridge. The second natural vibration has a frequency of 0.640Hz (the fifth mode in Table 1), which corresponds to the unique antisymmetric mode of arch bridges. This is lower than the 0.927Hz of the in-plane first symmetrical mode (the ninth mode in Table 1).

The first natural vibration of the out-of-plane natural vibration is the symmetrical mode. It has a natural frequency of 0.365Hz. An out-of-plane mode moves the two arch ribs in the reverse direction (the third mode in Table 1, 0.473Hz). This mode exists because only two lateral bracings are installed between the arch ribs and the stiffening girder and there is no lateral bracing in the center of the arch rib. Also there is a mode in which the movement of the stiffening girder is predominant, like the eighth mode of Table 1. This is due to the earthquake

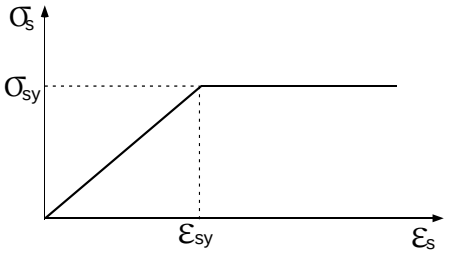

Figure 2: Stress-strain curve of steel tube

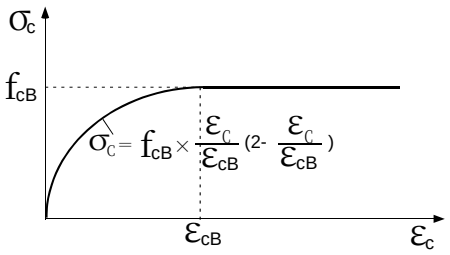

Figure 3: Stress-strain curve of infilled concrete

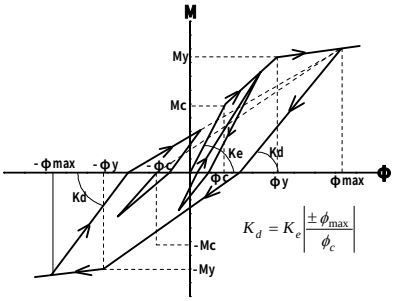

Figure 4: Takeda hysteretic property

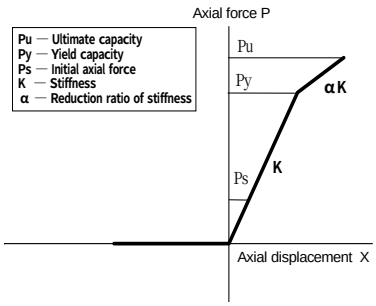

Figure 5: Nonlinear property of hangers

shear force distribution rubber bearings that are installed in the out-of-plane direction of the bridge.

5 NONLINEAR SEISMIC RESPONSE CHARACTERISTICS

5.1 Nonlinear seismic analysis and ground motions

In order to consider the material non-linearity used for the CFT arch ribs, the fiber model is adopted. This model can automatically take into account the axial force fluctuation and the non-linearity of biaxial bending moments. The elastic perfect plastic model[ix] for the steel tube is shown in Figure 2. The stress-strain curve proposed by Sato[xv], which takes into account the confinement of the infilled concrete, is used to determine the material non-linearity of the infilled concrete, as shown in Figure 3. The yield stress and yield strain are calculated using the following equations:

$$\text{Yield stress } f_{cB} = -\left\{\sigma_{ck} + 0.8(2t/D)\sigma_{sy}\right\} \tag{1}$$

$$\text{Yield strain } \varepsilon_{cB} = -\left(2.5 + 0.025\sigma_{ck}\right)\times 10^{-3} \ (\sigma_{ck} : \text{N/mm}^2) \tag{2}$$

where, σ_{sy} is the yield stress of the steel tube, σ_{ck} is the specified concrete strength, t is the thickness of the steel tube and D is the outer diameter of the steel tube.

The non-linearity of the piers is evaluated using the Takeda hysteretic model[xvi]. The restoring force characteristics (M-ϕ) of this model are shown in Figure 4. The hangers are modeled as members considering the effect of loosening. Figure 5 shows the relationship between the axial force and displacement of the hangers.

The nonlinear differential equations of motion of the bridge are directly integrated using

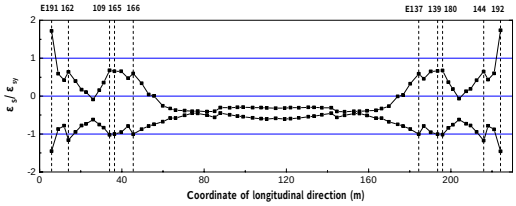

(a) Outside upper chord member

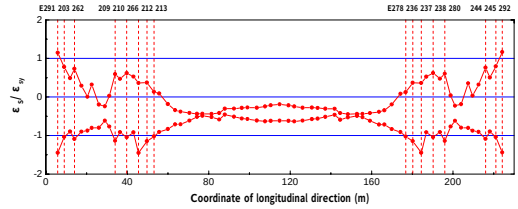

(b) Inside upper chord member

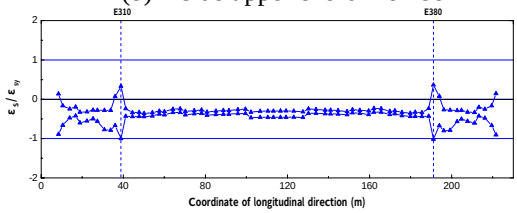

(c) Lower chord member

Figure 6: Maximum strains at the extreme edge of steel tubes

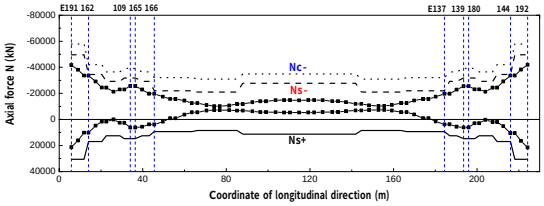

(a) Outside upper chord member

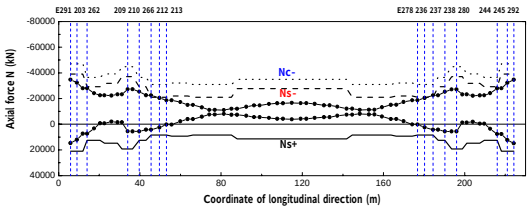

(b) Inside upper chord member

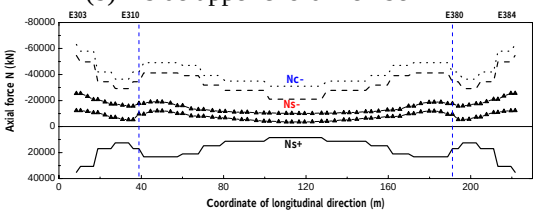

(c) Lower chord member

Figure 7: Maximum axial forces ***N***

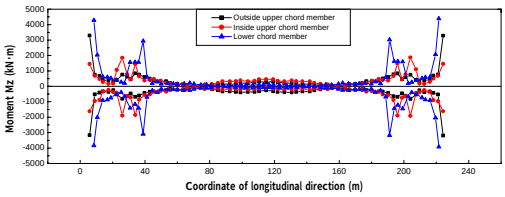

(a) Out-of-plane bending moment ***Mz***

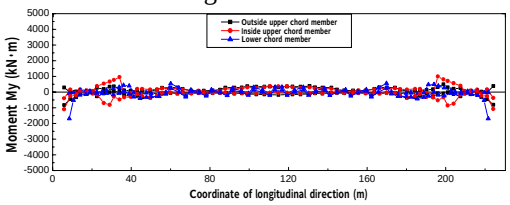

(b) In-plane bending moment ***My***

Figure 8: Maximum bending moment

the Newmark β method (β=0.25). The time interval of the numerical integration is 1/400 sec. The damping coefficients of all members are set to 0.02, and Rayleigh damping is employed. Two of the modes used in the Rayleigh damping are vibration with large effective masses. The first and fourth modes are employed for out-of-plane excitation, and the second and fifth modes are used for longitudinal excitation.

The ground motions used in this analysis are based on the Design Specification for Highway Bridges[ix]. They are standard strong earthquakes of Type I (T111, T112, T113) and Type II (T211, T212, T213) in the stiff soil condition. This bridge is located in the Kyushu Area, where strong earthquakes are rare. Therefore, the seismic zone coefficient is used to revise the input ground motions; this reduction coefficient is 0.7 according to Ref.[ix]. In other words, the seismic analysis applies seventy percent of the amplitude of the earthquakes.

The initial stress on the bridge is assumed to be that which is present under dead-load condition[xvii,xviii].

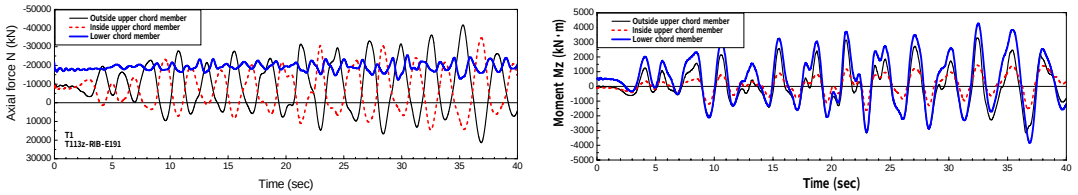

(a) Axial force ***N*** (b) Out-of-plane bending moment ***Mz***

Figure 9: Time histories of chord members at the springing position

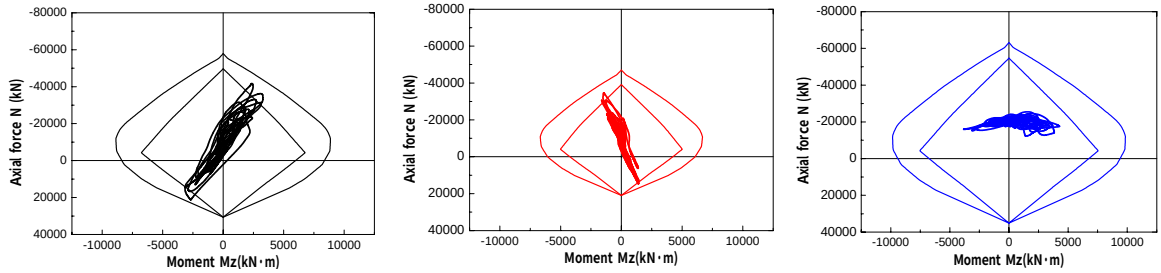

(a) Outside upper chord member (b) Inside upper chord member (c) Lower chord member

Figure 10: Correlation curve between axial force ***N*** and out-of-plane bending moment ***Mz***

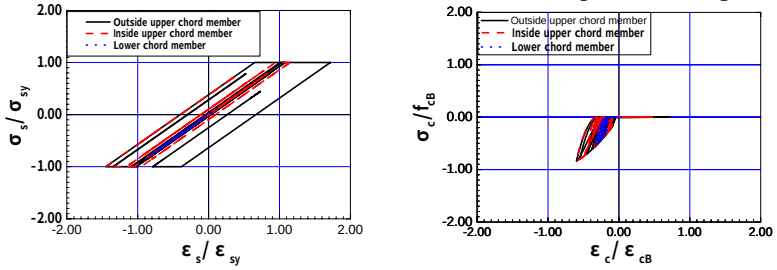

(a) Steel tube (b) Infilled concrete

Figure 11: Stress-strain curves of steel tube and infilled concrete at the springing position

5.2 Nonlinear response characteristics for out-of-plane excitation

When the bridge is subjected to T113 earthquake in the out-of-plane direction, the maximum strains at the extreme edge of the steel tubes are shown in Figure 6. The vertical axis shows the ratios of the strains to the absolute value of the yield strain of the steel tube, and the horizontal axis corresponds to the longitudinal coordinate of the bridge. The strains at the springing position and the joints between the arch rib and the stiffening girder are larger than those in the other parts. Furthermore, the strains in the upper chord members are larger than those in the lower chord member, and the strains of some elements of the upper chord members exceed the yield strains ($\varepsilon_s/\varepsilon_{sy}>1$, $\varepsilon_s/\varepsilon_{sy}<-1$).

In order to determine which stress resultant produced in these elements is predominant, the axial forces of the arch rib are examined first. Figure 8 shows the maximum axial forces. The yield axial forces N_s+ at which the axial forces of the steel tubes reach the plastic tensions, the yield axial forces N_s- at which the axial forces of the steel tubes reach the plastic compressive forces and the yield axial forces N_c- at which the axial forces of the infilled concrete member reach the plastic compressive force are also shown in Figure 7.

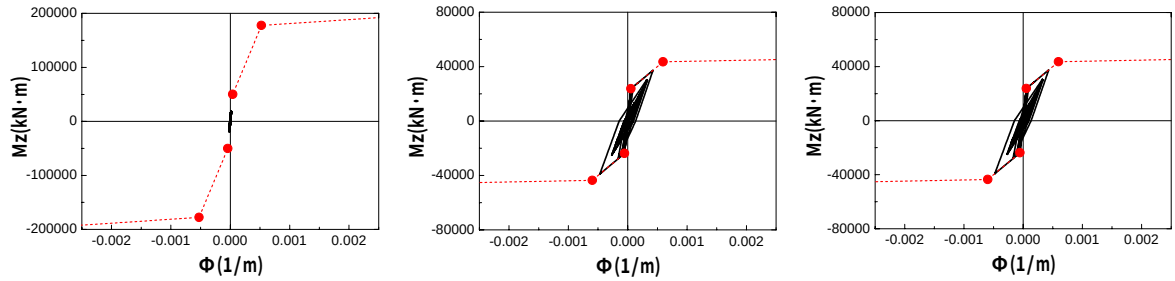

Pier P_4 Pier P_5 Pier P_6

Figure 12: M-ϕ curves of pier bases (T113 earthquake in the out-of-plane direction)

The axial forces of the lower chord member are smaller than those of the upper chord members. The axial forces of the upper chord member are generated in large amounts at the springing position and the joints between the arch ribs and the stiffening girder, and the axial force of element E266 exceeds the yield axial force N_s-. The steel tube of this element is a type STK400 tube with a thickness of t=14mm, therefore the yield axial force N_s- is small. It is also shown that the strain in this element exceeds the yield strain from Figure 6(a) for this steel tube.

There are elements other than element E266 in which the strains exceed the yield strains from the maximum strains listed in Figure 6(a), but these yielded elements cannot be determined from the maximum axial forces listed in Figure 7. It may be assumed that the bending moments that are generated in these elements are quite large.

Figure 8 shows the maximum out-of-plane bending moments Mz and the maximum in-plane bending moments My. When this bridge is subjected to a ground motion in the out-of-plane direction, the in-plane bending moments My are smaller than the out-of-plane bending moments Mz. In other words, the correlation of the biaxial bending moment of the arch rib does not need to be considered. Therefore, it seems possible to evaluate the response by using the correlation curve between the axial forces N and the out-of-plane bending moment Mz.

Time histories of the axial forces N and the bending moments Mz at the springing position of the three chord members are shown in Figure 9. Regarding element E303 of the lower chord member, the out-of-plane bending moment Mz is predominant even though the axial force N is small. The axial force N of element E191 of the outside upper chord members has the out-of-phase angle with that of element E291 of the inside upper chord members, and the out-of-plane bending moments Mz of these two elements have the same phase angle. These stress resultants of the upper chord members are applied as an out-of-plane bending moment Mz to the arch rib structure.

The correlation curves between the axial force N and the out-of-plane bending moment Mz at the springing position of the arch rib are shown in Figure 10. This figure also shows the first yield surface that the strains of the steel tubes at the extreme edge reach the yield strains of the steel tubes, and the second yield surface that the compressive strains of the concrete members at the extreme edge reach the yield strains of the infilled concrete. The bending moments of the elements at the springing position of the upper chord members exceed the first yield bending moment due to the large axial force N and the additional out-of-plane

bending moment Mz. As for the lower chord member, the out-of-plane bending moment Mz is predominant, and the elements remain elastic.

5.3 Nonlinear seismic response characteristics of piers

Figure 12 shows the M-ϕ curves of the bases of piers P4, P5 and P6. The curvature of pier P4 doesn't reach the crack curvature, while the curvatures of piers P5 and P6 exceed the crack curvature. The curvatures of the bases of piers P5 and P6 are configured so that they are within the permitted curvatures even though they reach the yield curvatures.

6 CONCLUSIONS

This paper examined the natural vibration and nonlinear seismic vibration of the Second Saikai Bridge, which is the first CFT arch bridge in Japan. The main findings were as follows:

- The unique antisymmetric mode of the arch bridge is the first in-plane vibration, and the symmetric mode is the first out-of-plane vibration.
- Regarding the yield characteristics of the arch rib, there are some elements whose axial forces exceed the yield axial force that axial forces of steel tubes reach plastic compressive forces, and some elements whose axial forces don't reach these yield axial forces. Strains in the steel tubes, however, exceed the yield strains of steel tubes due to an increase in the bending moment accompanied by a large axial force.
- Seismic safety can be confirmed because the strains in the infilled concrete of the arch rib do not reach to the yield strains and the curvatures of the piers are within the permitted curvatures.

REFERENCES

[i] C.W. Roeder, B. Cameron and C.B. Brown, Composite action in concrete filled tubes, Journal of Structural Engineering, ASCE, Vol.125, No.5, 477-484 (1999)

[ii] A.H. Varma, J.M. Ricles, R. Sause and L.W. Lu, Experimental behavior of high strength square concrete-filled steel tube beam-columns, Journal of Structural Engineering, ASCE, Vol.128, No.3, 309-318 (2002)

[iii] W.C. Clawson, Bridge Applications of Composite Construction in the U.S., Structural Engineering in the 21st Century, Proceedings of the 1999 Structures Congress, 544-547, (1999)

[iv] S. Nakamura, New structural forms for steel/concrete composite bridges, Structural Engineering International 1, Journal of the International Association for Bridge and Structural Engineering (IABSE), 45-50 (2000)

[v] Z. Zhen, B. Chen and Q. Wu, Recent Development of CFST Arch Bridge in China, Proceeding of 6th ASCCS Conference, pp.205-212 (2000)

[vi] Y. Liu, B. Chen and H. Hikosaka, Recent developments in concrete-filled tubular arch bridge and horizontal swing erection method in China, Bridge and Foundation Engineering, Vol.33, No.2, 41-44 (1999) (in Japanese)

[vii] Q. Wu, B. Chen, K. Takahashi and S. Nakamura, Construction and technical subjects of

concrete filled steel tubular arch bridges in China, Bridge and Foundation Engineering, Vol.35, No.10, 40-45 (2001) (in Japanese)
[viii] D. Peng, Q. Wu, K. Takahashi and S. Nakamura, Recent construction and development of long-span bridges in China, Bridge and Foundation Engineering, Vol.37, No.2, 43-49 (2003) (in Japanese)
[ix] Japan Road Association, Design Specifications for Highway Bridges, Part V: Seismic Design (1996) (in Japanese)
[x] Earthquake Engineering Committee of Japan Society of Civil Engineers, Earthquake Resistant Design Codes in Japan, Japan Society of Civil Engineering, Japan (2000)
[xi] Y. Liu, H. Hikosaka and B. Chen, Static characteristics and nonlinear seismic response of concrete-filled tubular arch bridge with half-though deck, Steel Construction Engineering, Vol.6, No.23, 53-61 (1999) (in Japanese)
[xii] Y. Liu, H. Hikosaka and B. Chen, Structural characteristic and seismic performance of steel-concrete composite tied arch bridge rigidly connected to piers, Journal of Structural Engineering, JSCE, Vol.47A, 1475-1484 (2001) (in Japanese)
[xiii] Y. Liu and H. Hikosaka, Assessment for ultimate strength and seismic performance of braced-rib arch bridge using concrete-filled tubes, Journal of Structure Mechanics and Earthquake Engineering, JSCE, No.703/I-59, 313-325 (2002) (in Japanese)
[xiv] Q. Wu, K. Takahashi, H. Matsuzaka, B. Chen and S. Nakamura, Study on dynamic properties of partially concrete filled steel tubular arch bridge, Journal of Constructional Steel, Vol.10, 141-148 (2002) (in Japanese)
[xv] T. Sato, Confining mechanism and analytical model in circular concrete-filled steel tube under axial force, Journal of Structure Construction Engineering, AIJ, No.452, 149-158 (1993) (in Japanese)
[xvi] T. Takeda, M.A. Sozen and N.N. Nielsen, Reinforced concrete response to simulated earthquakes, Journal of the Structural Division, ASCE, No.96, 2557–2573 (1970)
[xvii] W.X Ren and M. Obata, Elastic-plastic seismic behavior of long span cable-stayed bridges, Journal of Bridge Engineering, ASCE, Vol.4, No.3 (1999)
[xviii] H. Otsuka, Dynamic Design of Middle Span Bridges for Earthquake, Kyushu University Press, Japan (2000)